The Journal of Experimental Biology 210, 1183-1193
Published by The Company of Biologists 2007
doi:10.1242/jeb.000109

Scaling of contractile properties of catfish feeding muscles

Sam Van Wassenbergh[1,*], Anthony Herrel[1], Rob S. James[2] and Peter Aerts[1,3]

[1]*Department of Biology, Universiteit Antwerpen, Universiteitsplein 1, B-2610 Antwerpen, Belgium,* [2]*Department of Biomolecular and Sport Sciences, Coventry University, James Starley Building, Priory Street, Coventry, CV1 5FB, UK and* [3]*Department of Movement and Sports Sciences, Ghent University, Watersportlaan 2, B-9000 Gent, Belgium*

*Author for correspondence (e-mail: sam.vanwassenbergh@ua.ac.be)

Accepted 5 February 2007

Summary

Biomechanical models are intrinsically limited in explaining the ontogenetic scaling relationships for prey capture kinematics in aquatic vertebrates because no data are available on the scaling of intrinsic contractile properties of the muscles that power feeding. However, functional insight into scaling relationships is fundamental to our understanding of the ecology, performance and evolution of animals. In this study, *in vitro* contractile properties of three feeding muscles were determined for a series of different sizes of African air-breathing catfishes (*Clarias gariepinus*). These muscles were the mouth closer musculus adductor mandibulae A2A3′, the mouth opener m. protractor hyoidei and the hypaxial muscles responsible for pectoral girdle retraction. Tetanus and twitch activation rise times increased significantly with size, while latency time was size independent. In accordance with the decrease in feeding velocity with increasing size, the cycle frequency for maximal power output of the protractor hyoidei and the adductor mandibulae showed a negative scaling relationship. Theoretical modelling predicts a scaling relationship for *in vivo* muscle function during which these muscles always produced at least 80% of their maximal *in vitro* power. These findings suggest that the contractile properties of these feeding muscles are fine-tuned to the changes in biomechanical constraints of movement of the feeding apparatus during ontogeny. However, each muscle appears to have a unique set of contractile properties. The hypaxials, the most important muscle for powering suction feeding in clariid catfish, differed from the other muscles by generating higher maximal stress and mass-specific power output with increased size, whilst the optimum cycle frequency for maximal power output only decreased significantly with size in the larger adults (cranial lengths greater than 60 mm).

Key words: prey capture, size, muscle physiology, power, *Clarias gariepinus*.

Introduction

Increases in body size during the lifetime of animals have important implications for the mechanics of their musculoskeletal system (Hill, 1950; Schmidt-Nielsen, 1984; Biewener, 2005). When animals grow, their increased body size will generally impose different demands upon their morphology, behaviour and/or physiology. Because it is crucial to know how animals deal with the consequences of changes in size, studies of scaling relationships are fundamental to our understanding of the ecology, performance and evolution of animals (Herrel and Gibb, 2006).

One of the consequences of scaling is that larger aquatic suction-feeding vertebrates need a longer time to carry out a similar movement of their cranial system during prey capture (e.g. opening of the mouth or expansion of buccal cavity by the hyoid) compared with smaller animals of the same species (Richard and Wainwright, 1995; Reilly, 1995; Cook, 1996; Hernandez, 2000; Wainwright and Shaw, 1999; Robinson and Motta, 2002; Deban and O'Reilly, 2005; Van Wassenbergh et al., 2005a). A recent theoretical model (Van Wassenbergh et al., 2005a) calculated that for a 10-fold, isometric increase in size, the time needed to complete a rapid, size-proportional expansion of the bucco-pharyngeal cavity (which induces suction) increases by a factor of 4.64 [duration of kinematic events scale with length $(L)^{0.66}$]. In turn, as the time needed to draw prey towards and into the mouth cavity and the maximal distance from which prey can be caught depend on head size as well as the speed of feeding movements, these scaling relationships have important implications for the animal's success in capturing prey (Van Wassenbergh et al., 2006).

If the duration of head expansion is assumed to be size independent, the model (Van Wassenbergh et al., 2005a) predicts that the hydrodynamic resistance to expand the bucco-pharyngeal cavity will cause an increase in the required power by L^5 (pressure ~ L^2 × surface area ~ L^2 × linear velocity of expansion ~ L^1). This size-dependant resistance is primarily dictated by the forces needed to move head parts in the identical time frames against the pressure gradient between the inside

and the outside of the buccal cavity. However, similar to most other explosive movements – for example fast-starts for escaping predators (Wakeling and Johnston, 1998) – suction-feeding performance is most probably limited by the maximally available muscle power (Aerts et al., 1987; Carroll et al., 2004; Carroll and Wainwright et al., 2006). The underlying assumption of the model (Van Wassenbergh et al., 2005a) is that power output of the muscles that generate suction is directly proportional to the total mass of these muscles, and is hence proportional to L^3 (as that force is proportional to muscle cross-section, and contraction speed is proportional to fibre length). As a consequence of this mismatch between required and available power, isometrically growing animals must inevitably become slower in suction feeding during ontogeny.

As isometry also implies size-independent muscle strain (change in length divided by initial length), the slowing of suction feeding during ontogeny means that the relative speed of muscle contraction (muscle lengths per second) should decrease with size. This could have important consequences for the contractile physiology of the muscles powering feeding. It has been shown that in an ontogenetic series of aquatic animals, *in vitro* contractile properties of fast and slow muscles used in locomotion alter roughly in accordance with the speed of movement displayed *in vivo* (Anderson and Johnston, 1992; Altringham et al., 1996; James and Johnston, 1998; James et al., 1998) (but see Curtin and Woledge, 1988). However, to our knowledge, no data on the scaling of contractile properties of the fast-fibred muscles used for capturing prey are available in the literature. It is therefore unknown how animals precisely cope with the different dynamical environments imposed by the effects of scaling on the mechanics of the feeding system.

In the current study, we present the first data on scaling relationships of the contractile properties of muscles directly used for capturing prey. We analysed the contractile physiology of three muscles that are very important for powering prey capture in the African catfish *Clarias gariepinus* (Fig. 1), and presumably also for fish in general (e.g. Lauder, 1985): the hypaxial muscles, the protractor hyoidei and the adductor mandibulae A2A3′. By comparing theoretical scaling predictions of maximal speed of prey capture in catfish (Van Wassenbergh et al., 2005a) with *in vitro* contractile properties of the three feeding muscles from a range of catfish of different body sizes, we can test whether or how the contractile properties of these muscles are adjusted as a function of the biomechanical constraints of feeding causing the speed of muscle contraction to reduce during ontogeny.

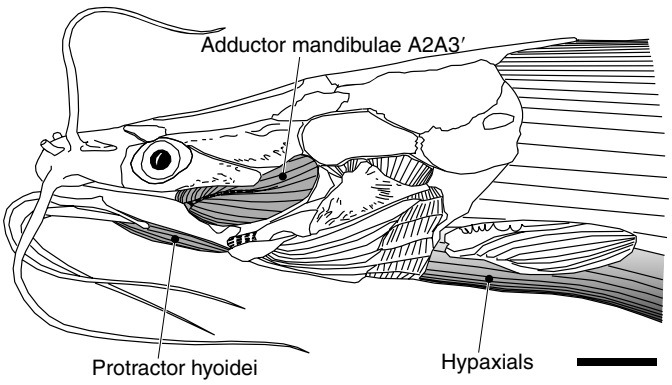

Fig. 1. Lateral view of the head of a juvenile *Clarias gariepinus* of 125.5 mm standard length [after Adriaens et al. (Adriaens et al., 2001)]. Indicated are the three muscles used in this study. Scale bar, 5 mm.

Materials and methods

Animals

Sixteen *Clarias gariepinus* (Burchell 1822) individuals between 14.4 and 205.4 mm in cranial length were used in this study. As the cranial length (defined as the distance between the rostral tip of the premaxilla and the caudal tip of the occipital process) can be measured more precisely and excludes variability in the length of body and tail, we used this metric to quantify size. Body mass varied from 1.83 g to 4770 g in this series of African catfish. Awaiting the experiments, all animals were kept in the same room at 22°C, each in a separate aquarium of which the dimensions were roughly proportional to the size of the fish. Each fish was killed by concussion of the brain by striking of the cranium, followed by destruction of the brain and transection of the spinal cord in accordance with the UK Home Office Animals (Scientific Procedures) Act 1986. The individuals used were either aquarium-raised specimens obtained from the Laboratory for Ecology and Aquaculture (Catholic University of Leuven, Belgium) or specimens obtained from aquaculture facilities (Fleuren & Nooijen BV, Someren, The Netherlands). However, catfish from both origins did not show different growth patterns of the feeding apparatus (Herrel et al., 2005). This species was chosen because scaling relationships of morphology (Herrel et al., 2005) and prey capture kinematics (Van Wassenbergh et al., 2005a), as well as a more detailed study on functioning of the cranial system (Van Wassenbergh et al., 2005b), are available in the literature and can thus be used to interpret the results. Also, individuals of different sizes were readily available.

Muscle preparations

Three muscles were studied (Fig. 1): (1) the hypaxials (abbreviated m-hyp), the most important muscle for powering head expansion in clariid catfish; (2) the musculus protractor hyoidei (abbreviated m-pr-h), functioning as a mouth opener in *C. gariepinus* (see Van Wassenbergh et al., 2005b) and (3) the musculus adductor mandibulae A2A3′ (abbreviated m-a-m), the largest part of the jaw adductor muscle complex, responsible for closing the mouth rapidly and exerting bite force onto prey. From this point on, the abbreviations m-hyp, m-pr-h and m-a-m will be used to refer to these muscles (see also Fig. 1). The m-pr-h and m-a-m of a single side were dissected as a whole, leaving it attached to the part of the bones that serve as the muscle's origin and attachment. The anterior part of the m-hyp was dissected out. Next, the muscle

preparations were transferred to a Ringer solution maintained at 4°C. The composition of the Ringer solution used in the present study is identical to the one used for *Cyprinus carpio* (Wakeling and Johnston, 1999). Small bundles of m-hyp muscle fibres were dissected from the anterior part of the m-hyp using a dissecting stereoscope. The resulting m-hyp muscle preparations always originated from approximately one-third of the animal's cranial length posterior to the medial attachment with the cleithrum.

The bone at either end of the muscle preparation was clamped *via* crocodile clips to a strain gauge (UF1; Pioden Controls Ltd, Inverness, UK) at one end and a motor arm (V201; Ling Dynamics Systems, Herts, UK) attached to an LVDT (Linear Variable Displacement Transformer; DFG 5.0; Solartron Metrology, Leicester, UK) at the other. Meanwhile, the preparation was placed into a flow-through chamber of oxygenated Ringer solution that was kept between 26.8 and 27.2°C (close to the optimum temperature used for breeding *C. gariepinus*) (Hossain et al., 1999). For the m-hyp bundles, aluminium foil T-shaped clips were folded over the myoseptum at both ends of the muscle fibre bundle, and these foil clips were clamped into the crocodile clips, as detailed above. Electrical stimulation was delivered *via* a pair of platinum electrodes running parallel to the muscle preparation.

Isometric contractile properties

The length of the preparation was adjusted to give maximal twitch force, thereby putting the sarcomeres close to their optimal length for maximal force production (Rome and Sosnicki, 1991). The length at which the muscle produced maximal force (L_0) was measured using digital calipers (±0.1 mm). Stimulation amplitude and pulse width were also adjusted to maximize twitch force. A pulse width of 1.5 ms was used. Stimulation frequency was adjusted to maximize tetanus height. In order to allow accurate quantification of rise times, tetanus stimulations were sustained for 150 ms for the m-hyp and 300 ms for the m-pr-h and m-a-m. A recovery time of 5 min was allowed between each tetanus. Latency (time between the onset of stimulation and the start of force production), time to peak twitch force and time to 50% of peak tetanus force were measured to indicate the rate of force increase.

In vitro power output

The work loop technique (Josephson, 1985) was used to measure power output of the muscles subjected to sinusoidal cycles of lengthening and shortening about L_0. A sinusoidal strain waveform with a total strain of 10% of L_0 (±5%) was imposed during the experiments, as this approximates the *in vivo* shortening pattern measured for the m-pr-h by high-speed X-ray video of *C. gariepinus* during prey capture (Van Wassenbergh et al., 2005b). Using the model of Van Wassenbergh et al. (Van Wassenbergh et al., 2005c), we calculated that a 10% strain in the m-a-m corresponds to the situation in which the mouth is closed from a gape angle of 47°, which is relatively high, but perfectly feasible for this species. Because no data are available on strain amplitude of the m-hyp during feeding, we used the same shortening–lengthening regime as for the other two muscles to enable direct comparison (10% sinusoidal strain).

Muscles were subjected to sets of four cycles of active work loops, of which the second cycle was selected for further analyses. Note that relatively small differences were observed between the consecutive cycles: maximal net contractile power for the second cycle in a random sample of 10 sequences from the m-hyp, m-pr-h and m-a-m are 92±5%, 97±6% and 103±16% (mean ± s.d.), respectively, of the first cycle. A recovery time of 5 min was allowed between each work loop run. The net power per cycle, however, is a complex function of strain, cycle frequency, number and timing of stimuli (Altringham and Johnston, 1990). Therefore, in order to analyze the optimum cycle frequency for producing power, each preparation was subjected to at least six different cycle frequencies. The number of stimuli per cycle and the stimulation phase (timing of stimulation) was varied at each cycle frequency to maximize power output. To monitor progressive changes in contractile performance, the conditions used at the first cycle frequency were repeated after every three sets of work loops. A loss of about 15% in power output was typically observed after six consecutive sets of work loops, which is presumably caused by some fibres becoming inexcitable. Any loss in power output was due to a reduction in force production during the work loop, rather than a change in work loop shape. To correct for this deterioration in muscle power output, a linear interpolation of power loss-percentage as a function of time was used.

At each cycle frequency, the muscle was subjected to a set of four passive work loops, i.e. without electrical stimulation. These passive force values (from passive work loops) were subtracted from the corresponding active forces (from any active work loops at the same cycle frequency) to give the active contractile force (Fig. 2A,C). Instantaneous power was calculated as the product of this contractile force and the velocity of movement. Average power in each movement cycle was calculated as the instantaneous contractile power averaged over the entire movement cycle. All power outputs subsequently reported are those averaged across a full work loop cycle. A zero phase-shift, fourth-order low-pass Butterworth filtering of the measured force and length data was applied to reduce noise in the work loops (Fig. 2A). A standard cut-off frequency of 60 times the sampling frequency was used, followed by a graphical check and (if necessary) an adjustment of the cut-off frequency to achieve adequate filtering.

After the experiments, muscle tissue was dissected from the preparation and muscle mass was determined (±0.01 mg). Any dead fibres were removed from the outer edges of the muscle to ensure that any muscle fibres damaged during dissection were removed. Cross-sectional area was calculated by dividing muscle volume (assuming a density of 1060 kg m^{-3}) (Mendez and Keys, 1960) by L_0. Maximal isometric stress was calculated by dividing maximal force by cross-sectional area. Maximal normalized power output was calculated relative to

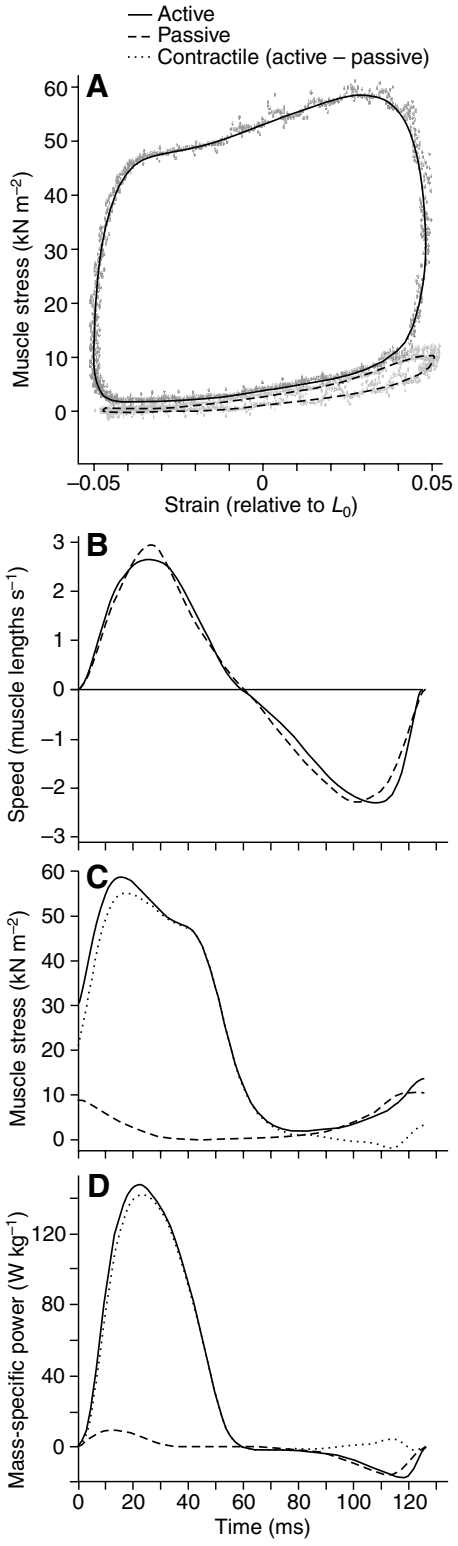

Fig. 2. Example of a work loop (A) generated during 8 Hz sinusoidal length changes (strain of 10%) for the musculus protractor hyoidei (m-pr-h) of an 80.1 mm cranial length *C. gariepinus*, with (B) the corresponding instantaneous relative speed, (C) force per muscle cross-sectional area and (D) muscle-mass-specific power output. In A, raw data points are shown as well as the work loop curve after Butterworth filtering. The force produced by only the actively contracting components of the muscle was calculated by subtracting the force measured without stimulation (passive work loop) from the force with stimulation (active work loop).

wet mass to take account of differences in size of muscle preparations. The proportion of connective tissue within the muscles is assumed not to change with body size or differ between muscles used in this study. However, as connective tissue has relatively low density and is a small proportion of the muscle volume, this assumption seems justified since potential differences will probably have a small effect on muscle density.

Values of maximal force and power were discarded for any muscle preparation that failed to generate above 20 kN m^{-2} during tetanic stimulation. This occurred in seven out of 48 muscles that were analyzed, without displaying a correlation with the size of the animals studied (m-hyp, 16.0, 205.4 mm; m-pr-h, 16.0 mm; m-a-m, 16.0, 21.0, 190.0, 205.4 mm cranial length). It is assumed that these discarded preparations had a large fraction of the muscle fibres that had died between the time of sacrificing the animal and placing the dissected muscle into the Ringer solution. The data for these preparations clearly fell below the lower 95% confidence interval of the rest of the data, which further reassured us that the results from these preparations were not representative of the rest of the collected data. Our impression was also that any muscle preparation that produced less than 20 kN m^{-2} stress underwent rapid deterioration in contractile performance.

It should be noted that cyclic length changes imposed on the muscle preparations, as performed in the present study, might not always be the most ideal condition for mimicking the *in vivo* behaviour of feeding muscles. Nevertheless, the m-a-m will inevitably be stretched prior to mouth closing, and consequently has a clear eccentric phase and an overall strain pattern approximately similar to the sinusoidal waveform of lengthening–shortening imposed in the presented *in vitro* experiments. A short eccentric phase of relatively small amplitude and an approximately overall sinusoidal strain pattern can also be recognized for the m-pr-h during prey capture in *C. gariepinus* (Van Wassenbergh et al., 2005b). However, for the post-cranial muscles used for pectoral girdle retraction or neurocranial elevation (e.g. m-hyp), measuring power output when activation starts during lengthening may not be fully representative of the *in vivo* situation in which activation of the muscles is normally followed by a concentric contraction (Carroll and Wainwright, 2006; Coughlin and Carroll, 2006). However, given the purpose of the present study, i.e. analyzing scaling effects on contractile properties, it is very unlikely that this could have influenced the observed scaling relationships (more specifically, the slopes of log–log regressions). Furthermore, using also the work loop technique for the m-hyp has the important advantage of enabling comparison between the different feeding muscles and

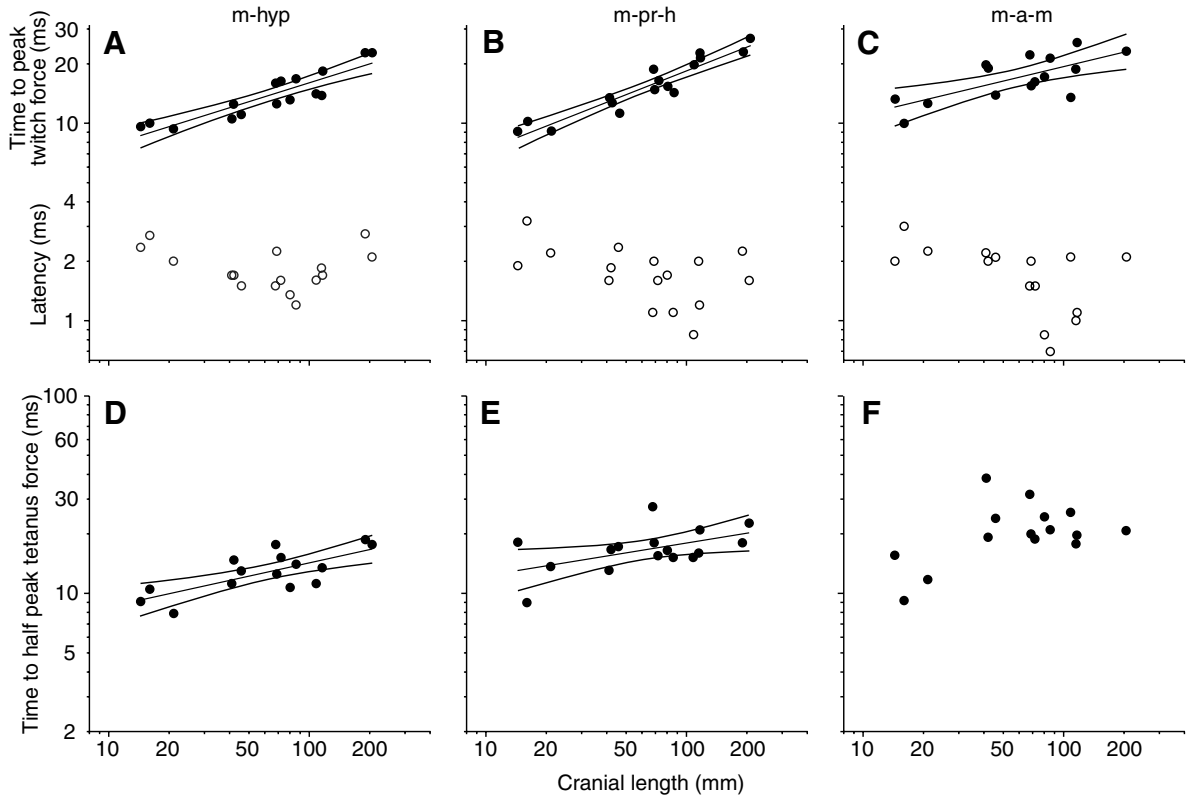

Fig. 3. Log–log plots of latency (open circles), time to peak force during twitch stimulation (full circles; A–C) and time to half peak force during tetanus stimulation (D–F) *versus* cranial length. The muscle names are indicated above the graphs. See Table 1 for linear regression statistics. Abbreviations: m-a-m, musculus adductor mandibulae A2A3′; m-hyp, hypaxials; m-pr-h, protractor hyoidei.

comparison with most of the data available in the literature on other types of muscle (e.g. muscles used for locomotion).

Relationships between cycle frequency and power output

The maximized contractile power outputs of at least six work loops of differing cycle frequency were plotted against cycle frequency. A third-order polynomial fit was used to determine the cycle frequency for maximal power output. Power output values were then expressed as a percentage of maximum power, and ranges were determined for cycle frequencies yielding at least 90%, 80% and 70% of this maximum.

Scaling relationships of the cycle frequency for maximal power output were compared to a model prediction of scaling relationships for *in-vivo* shortening speed of the m-pr-h and m-a-m in *C. gariepinus* during prey capture. The inverse dynamical model by Van Wassenbergh et al. (Van Wassenbergh et al., 2005a) accounts for the allometry in muscle mass in this species (assumed to influence mass-specific power output) as measured by Herrel et al. (Herrel et al., 2005) and predicts that movement durations increase with the animal's head length (L) by $L^{0.53}$. High-speed X-ray video data on shortening speeds of the m-pr-h and m-a-m (Van Wassenbergh et al., 2005b) were used to determine the intercept for the scaling regressions. To do so, for each of the three individuals studied by Van Wassenbergh et al. (Van Wassenbergh et al., 2005b), five feeding sequences in which the strain was closest to 10% were selected. The reciprocal of twice the average duration of the shortening phase was used as a measure for sinusoidal strain cycle frequency. Finally, scaling regressions were plotted through the point in which cranial length and frequency were averaged for the three individuals.

Statistics

All data were $\log_{10}$ transformed (one data point for each individual) and were plotted against the $\log_{10}$ of cranial length. Next, least-squares linear regressions were performed on these data. As the measured physiological variables (dependent data) are likely to have a much greater error than measurements of cranial length (independent data), least-squares regressions are appropriate in this case (Sokal and Rohlf, 1995). The slopes of these linear regressions with 95% confidence limits were determined in order to evaluate changes in contractile properties of the muscles in relation to changes in body size. Note that a near-isometrical relationship exists between cranial length and body mass (log–log regression slope of 2.96, r^2=0.99), implying identical scaling results if the cube root of body mass would have been used to quantify size.

Each linear regression was tested for statistical significance by an analysis of variance (ANOVA). To compare the observed regression slopes against model predictions, the significance of the regressions after rotating the frame of reference of the data with respect to the predicted slope, which becomes parallel to

Table 1. *Scaling relationships of contractile properties of feeding muscles in C. gariepinus*

	Slope	r^2	95% confidence limits of slope		Intercept	95% confidence limits of intercept		P	N	Mean ± s.d.* or range
Latency (ms)										
m-hyp	–0.062	0.04	–0.230	0.105	0.371	0.065	0.676	0.44	16	1.9±0.5
m-pr-h	–0.193	0.21	–0.409	0.024	0.574	0.179	0.969	0.077	16	1.8±0.6
m-a-m	–0.279	0.26	–0.559	0.000	0.706	0.205	1.207	0.050	15	1.8±0.6
Time to peak twitch force (ms)										
m-hyp	0.318	0.80	0.228	0.409	0.569	0.405	0.734	**<0.0001**	16	9.4–22.8
m-pr-h	0.401	0.89	0.321	0.482	0.471	0.324	0.618	**<0.0001**	16	9.2–27.2
m-a-m	0.244	0.50	0.099	0.389	0.799	0.540	1.059	**0.003**	15	10.0–25.6
Time to half peak tetanus force (ms)										
m-hyp	0.222	0.54	0.105	0.340	0.710	0.496	0.925	**0.001**	16	7.9–18.8
m-pr-h	0.162	0.27	0.011	0.314	0.929	0.653	1.206	**0.038**	16	9.0–27.5
m-a-m	0.230	0.25	–0.008	0.469	0.896	0.470	1.323	0.057	15	21±7
Maximal isometric stress (kN m^{-2})										
m-hyp	0.748	0.70	0.441	1.055	0.643	0.075	1.218	**0.0002**	14	35–453
m-pr-h	0.593	0.51	0.245	0.940	1.082	0.437	1.728	**0.003**	15	32–281
m-pr-h (excl. two smallest fish)	0.228	0.11	–0.208	0.664	1.811	0.967	2.655	0.27	13	188±62
m-a-m	–0.044	0.00	–0.689	0.600	2.343	1.187	3.499	0.88	11	203±87
Cycle freq. for max. power (Hz)										
m-hyp	–0.105	0.15	–0.246	0.036	1.391	1.134	1.649	0.13	16	16±3
m-hyp (>60 mm CL)	–0.536	0.79	–0.758	–0.314	2.275	1.827	2.723	**0.0005**	10	10.5–21.0
m-pr-h	–0.377	0.89	–0.453	–0.301	1.649	1.510	1.788	**<0.0001**	16	5.5–17.0
m-a-m	–0.333	0.58	–0.502	–0.164	1.466	1.163	1.768	**0.0009**	15	3.5–13.0
Maximal power (W kg^{-1})										
m-hyp	0.620	0.57	0.279	0.961	0.541	–0.098	1.180	**0.002**	14	15.8–120.3
m-pr-h	0.451	0.49	0.173	0.730	0.730	0.833	0.316	**0.004**	15	12.4–83.4
m-pr-h (excl. two smallest fish)	0.149	0.09	–0.160	0.459	1.438	0.839	2.037	0.31	13	55±14
m-a-m	–0.063	0.01	–0.591	0.465	1.742	0.795	2.688	0.79	11	46±17

P-values of significant scaling relationships (P<0.05) are indicated in bold. Abbreviations: CL, cranial length; m-hyp, hypaxials; m-pr-h, protractor hyoidei; m-a-m, adductor mandibulae A2A3′.

*Means ± s.d. are only given in cases where there is no significant scaling relationship.

the new x-axis, was tested by ANOVA. Differences between the muscles in the scaling regression slopes for a given variable were tested (F-test of interactions by covariates) using cranial length as a covariate in an analysis of covariance (ANCOVA). Only if these slopes did not differ significantly (P>0.05) could differences in the intercept for the different muscles be evaluated statistically without violating the ANCOVA assumption of parallelism.

Results

Latency and rise times of isometric contractions

No significant scaling relationships were observed in the time between the onset of stimulation and muscle force output (Fig. 3; Table 1). Furthermore, this latency time did not differ between the three muscles (ANCOVA, $F_{2,41}$=1.1, P=0.34). The mean latency of the entire data set was 1.8±0.6 ms (mean ± s.d.).

The times to peak twitch force increased significantly with size for each of the three muscles (Fig. 3; Table 1). Values approximately doubled from the smallest to the largest fish used in this study. The scaling relationships (regression slopes) for this variable did not differ significantly between the muscles (ANCOVA, $F_{2,41}$=2.5, P=0.09). However, after eliminating size effects, twitch rise times differed significantly between the muscles (ANCOVA, $F_{2,43}$=8.5, P=0.0008). A pairwise comparison showed that the m-hyp had a significantly shorter twitch rise time compared with the m-pr-h (ANCOVA, $F_{1,29}$=6.95, P=0.013) and, even more pronounced, compared to the m-a-m (ANCOVA, $F_{1,28}$=14.7, P=0.0007). The m-pr-h did not differ significantly with the m-a-m in the time to peak twitch force (ANCOVA, $F_{1,28}$=3.4, P=0.08).

The times to half peak tetanus force also increased significantly with size for the m-hyp and m-pr-h (Fig. 3; Table 1) but not for the m-a-m (P=0.057; Table 1). Similar to the twitch rise times, significant differences between the muscles were observed for the rise times during tetanus activation (ANCOVA, $F_{2,43}$=14.8, P<0.0001). Also, the scaling relationships (regression slopes) were not statistically different between the muscles (ANCOVA, $F_{2,41}$=0.2, P=0.8). Again, the

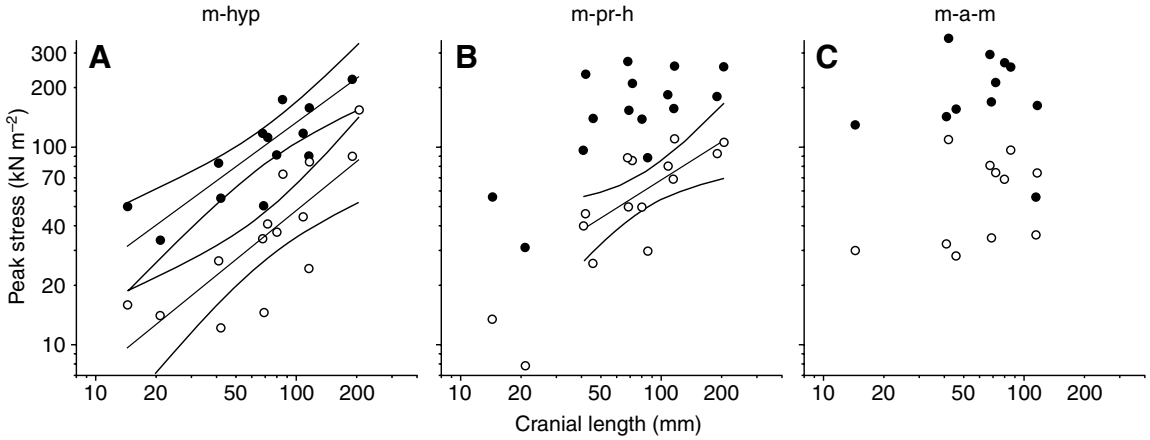

Fig. 4. (A–C) Log–log plots of peak force per muscle cross-sectional area during twitch (open circles) and tetanus stimulation (full circles) *versus* cranial length. The muscle names are indicated above the graphs. Data on m-pr-h force of the smallest two individuals are excluded from the regression analysis. See Table 1 for regression statistics. Abbreviations: m-a-m, musculus adductor mandibulae A2A3′; m-hyp, hypaxials; m-pr-h, protractor hyoidei.

m-hyp had the fastest tetanus rise time. The m-pr-h was intermediate between the m-hyp and the m-a-m and differed significantly from both muscles (ANCOVA, $F_{1,29}$=14.2, P=0.0008; $F_{1,28}$=4.45, P=0.044, respectively).

Maximal isometric stress

Maximal force per cross-sectional area of the muscle increased continuously with size for the m-hyp (Fig. 4A; Table 1) in both twitch and tetanus responses. Although the same overall trend can be observed for the m-pr-h (Fig. 4B; Table 1), no significant scaling relationship could be demonstrated if the two smallest individuals in the study were excluded from the regression analysis. In contrast to the m-hyp, the maximal isometric force of the m-a-m did not increase significantly during ontogeny (Fig. 4C; Table 1).

Power output–cycle frequency relationships

The cycle frequency for maximal power output was independent of size for the m-hyp (Fig. 5A; Table 1) but decreased significantly during ontogeny for the m-pr-h and the m-a-m (Fig. 5B,C; Table 1). As a consequence, the scaling relationship of optimum shortening velocity for producing power differed significantly between the muscles used in the present study (ANCOVA, $F_{2,41}$, P=0.006). The

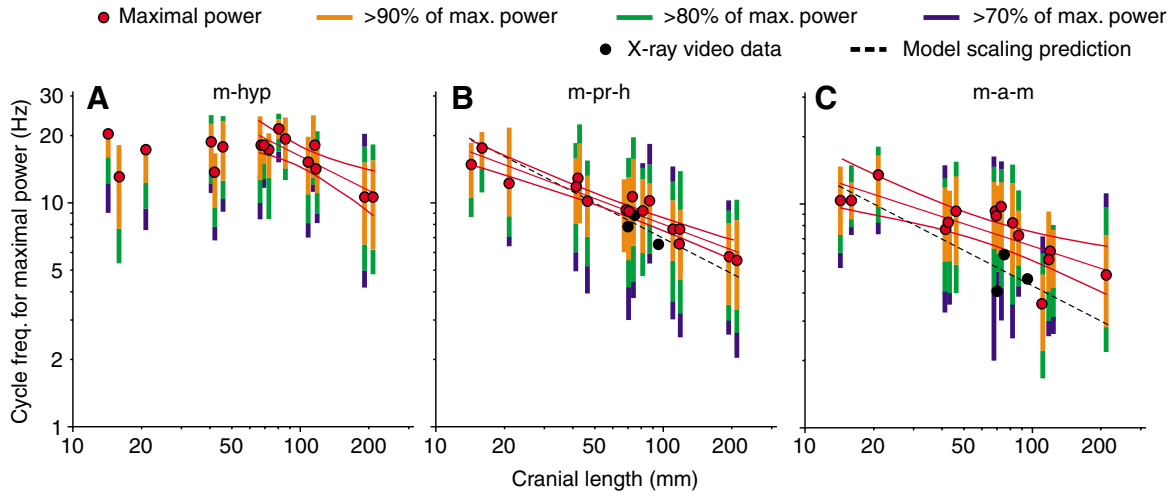

Fig. 5. (A–C) Log–log plots of cycle frequency for maximal muscle power output *versus* cranial length. Observations of *in vivo* cycle frequency for three individuals inferred from high-speed X-ray videos are also shown (black circles). The scaling relationship predicted by inverse dynamic suction modelling (speed scales with $L^{-0.533}$) (Van Wassenbergh et al., 2005a) is also illustrated (black line). Note the apparent breakpoint in the scaling relationship for the m-hyp (A) in which only fish greater than 60 mm show a significantly negative slope in this scaling relationship. Since no data on *in vivo* m-hyp strain during feeding are available, the intercept of the scaling regression predicted by modelling could not be determined in A. Table 1 gives additional regression statistics. Abbreviations: m-a-m, musculus adductor mandibulae A2A3′; m-hyp, hypaxials; m-pr-h, protractor hyoidei.

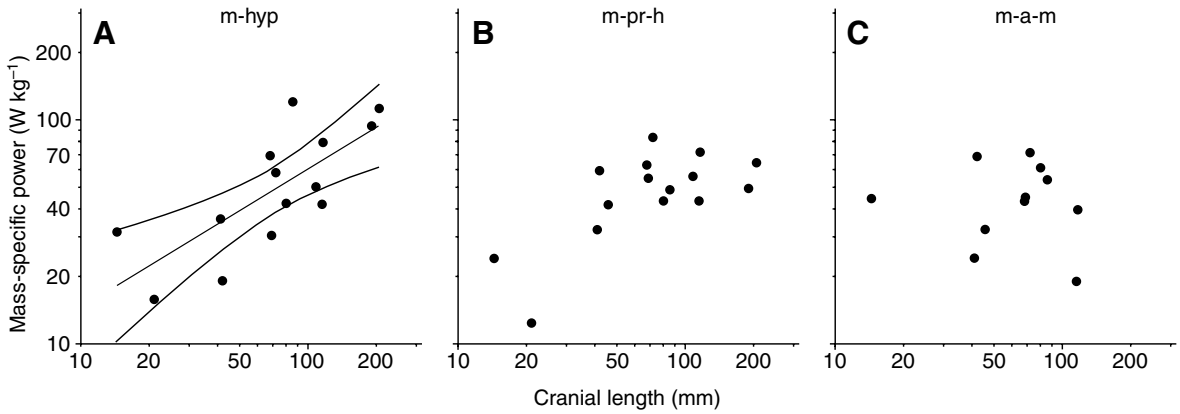

Fig. 6. (A–C) Log–log plots of maximal muscle-mass-specific power *versus* cranial length. The muscle names are indicated above the graphs. Data on m-pr-h force of the smallest two individuals are excluded from the regression. See Table 1 for regression statistics. Abbreviations: m-a-m, musculus adductor mandibulae A2A3′; m-hyp, hypaxials; m-pr-h, protractor hyoidei.

slopes of the regressions for the m-pr-h (Fig. 5B) and the m-a-m (Fig. 5C) did not differ significantly (ANCOVA, $F_{1,27}$=0.28, P=0.6). The cycle frequency for generation of maximal power output of the m-a-m was, irrespective of size, significantly lower than that measured for the m-pr-h (ANCOVA, $F_{1,28}$=15.3, P=0.0005).

However, a closer inspection of the power-output–cycle frequency relationship for the m-hyp (Fig. 5A) suggested the presence of a breakpoint at a cranial length of ~60 mm. For fish with cranial lengths greater than 60 mm, the cycle frequency for maximal power output decreases significantly (P=0.0005) with a slope of –0.54±0.10 (N=10, r^2=0.79). Below the breakpoint, this scaling relationship is size-independent (slope=–0.01±0.17; N=6, r^2=0.00, P=0.98). The approximate position of the breakpoint was indicated by a sudden increase in r^2 at this point after one-by-one removal of the smallest individuals from the data set.

The cycle frequency for maximal power output decreased with size significantly less rapidly than expected on the basis of the model calculations for the m-pr-h and for the m-hyp of fish smaller than 60 mm in cranial length (both P<0.0007; Fig. 5A,B). On the other hand, no significant differences between model prediction (slope of –0.533) and the measured slope are observed for the m-a-m (P=0.95) or the m-hyp of fish greater than 60 mm (P=0.98). This scaling relationship predicted by modelling stays within the plateau region where 90% and 80% of the optimum power is produced, respectively, for the m-pr-h and the m-a-m (Fig. 5B,C).

No significant differences between the scaling slopes of the three muscles are found if the m-hyp data of only the fish greater than 60 mm are considered (ANCOVA, $F_{2,35}$=0.97, P=0.39). However, after eliminating size effects, cycle frequencies for maximal power output differed significantly between the muscles (ANCOVA, $F_{2,37}$=93.3, P<0.0001). A pairwise comparison showed that the m-hyp had a significantly higher cycle frequency for maximal power output compared with the m-pr-h (ANCOVA, $F_{1,23}$=205.4, P<0.0001). In turn, the m-pr-h shows a significantly higher cycle frequency for maximal power output compared with the m-a-m (ANCOVA, $F_{1,23}$=15.3, P=0.0005).

Maximal in vitro power output

The scaling relationships of the *in vitro* maximal mass-specific power output (Fig. 6) were similar to the results for maximal tetanus force per cross-sectional area of the muscle (Fig. 4). Power output increased significantly during ontogeny for the m-hyp (Fig. 6A; Table 1) and also for the m-pr-h during the juvenile developmental stages (Fig. 6B). By contrast, mass-specific power output was independent of size for the m-a-m (Fig. 6C), and also for the m-pr-h for *C. gariepinus* individuals approximately larger than 40 mm in cranial length (Fig. 6B).

Discussion

The feeding system of animals is crucial to their survival. Feeding performance strongly depends on the muscles that drive the motions of the feeding apparatus. The results of the present study show that body size, and the biomechanical implications thereof, is not only manifested at the level of feeding kinematics (e.g. Richard and Wainwright, 1995; Wainwright and Shaw, 1999; Meyers et al., 2002; Robinson and Motta, 2002), dynamics (Van Wassenbergh et al., 2005a; Wainwright et al., 2006) or allometric growth patterns (e.g. Hernandez and Motta, 1997; Herrel et al., 2005) but also in the physiological characteristics of the muscles.

Logically, in order to optimize performance, the contractile properties of muscles should be tuned to the contractile regime of the muscle. Hill pointed out that differences in body size between animals cause a strong need for changes in contractile characteristics to match alterations in functional demands (Hill, 1950). Relative speed of limb movement, for example, differs greatly between mouse and horse, and so does the contractile physiology of their limb muscles (Medler, 2002).

However, large differences in body size are not only found when comparing different species but also during ontogeny of animals like *C. gariepinus* and many other ectotherms, where

length and mass increase several orders of magnitude. In these animals, the muscular properties must be fine-tuned during growth in order to reach a situation in which the muscles can work under their optimal contractile regime. As developmental constraints are involved in this process, ontogenetic studies are not identical to interspecific comparisons.

Yet, ontogenetic studies of contractile properties of fish swimming muscles (Anderson and Johnston, 1992; James et al., 1998) have shown that isometric activation times are significantly longer in larger fish, and the cycle frequency for maximal power output reduced when fish increase in size (Altringham and Johnston, 1990; Anderson and Johnston, 1992). In the present study, we see a similar trend for the fast-fibred feeding muscles of *C. gariepinus* (Figs 3, 5). Especially for the m-pr-h, the muscle used for opening the mouth, the *in vitro* observations for the cycle frequency for maximal power output are, as expected, very close to the direct *in vivo* measurements of shortening velocity during prey capture (Fig. 5B). These findings suggest that the contractile physiology of the m-pr-h is well-adapted to produce maximal power during suction feeding. The *in vitro* power optimum for the m-a-m, the mouth-closer and biting muscle, appears to be reached at slightly higher shortening speeds than the ones inferred by modelling based on high-speed X-ray video data (Fig. 5C). Nevertheless, both muscles' scaling relationships of speed *versus* cranial length predicted by modelling (Van Wassenbergh et al., 2005a) fall entirely within the range of 80% of the optimum power generation for the complete range of sizes used in the present study. This suggests that the theoretical predictions of scaling of feeding kinematics are in close accordance with the contractile properties of the muscles used for powering feeding in the African catfish.

A critical assumption in studies trying to explain the scaling of feeding kinematics and performance (Van Wassenbergh et al., 2005a; Van Wassenbergh et al., 2006) is that the power output of a muscle scales with the mass of this muscle (i.e. constant muscle-mass-specific power). Our data show that this holds true for the m-pr-h (excluding the juveniles smaller than 20 mm cranial length; Fig. 6B) and the m-a-m (Fig. 6C). Even if we account for the slowing down of contraction speed of the muscles with increasing catfish size, the observed scaling relationships of optimum-power–cycle frequency (Fig. 5; Table 1) has very little influence on this mass-specific power output because of the relatively small difference from the predicted scaling relationship (angular speed proportional to cranial length$^{-0.533}$) (Van Wassenbergh et al., 2005a).

Remarkably, the m-hyp shows different scaling relationships from the m-pr-h or the m-a-m (Table 1). As maximal stress of the m-hyp increases significantly with size (Fig. 4A), the intrinsic properties might still be under development until the late adult stages. A study of the expression of myosin isoforms could potentially explain this unexpected result. It should be noted that the power output of this muscle already reaches approximately the level of the other two muscles (m-pr-h and m-a-m) at fish with head sizes of 30 mm. The highest values for power output are also measured for the m-hyp (Fig. 6). Consequently, except for the smaller juveniles, the crucial role of the m-hyp for generating suction power is well supported by the physiological data.

Rather unexpectedly, the m-hyp of juveniles and smaller *C. gariepinus* adults (cranial length smaller than 60 mm) differs from the other muscles in its size independence in the cycle frequency for maximal power output (Fig. 5A). This scaling relationship changes for the m-hyp of the larger fish, which show the more general decrease in cycle frequency for maximal power output with increasing size (see Fig. 5). Unfortunately, too little is known about the *in vivo* contractile behaviour of the m-hyp to explain these results. From a functional point of view, there is a fundamental difference between the m-hyp and muscles like the m-pr-h and the m-a-m. While the latter muscles have a clear origin and insertion, the m-hyp in *C. gariepinus* and nearly all other fish continues posterior into the ventral body musculature (Diogo et al., 2001). Activation patterns in the epaxials, a muscle similar to the m-hyp in this respect, are not spatially uniform; muscle activation intensity recorded for the anterior region of the epaxials is consistently higher than from the more posterior region in the percomorph fish, *Micropterus salmoides* (Thys, 1997). This implies that patterns of strain and strain rate within muscles like the epaxials and hypaxials can also be spatially non-uniform. Furthermore, the m-hyp is not only used for feeding but also contributes to the lateral undulation during swimming (e.g. Altringham and Ellerby, 1999). The difference in the scaling relationships of the m-hyp compared with the other muscles may therefore be a result of the dual function of this muscle and the consequent potentially different developmental constraints involved.

Small differences in intrinsic contractile properties such as twitch and tetanus times and maximal shortening velocities (Fig. 3) do not necessarily have biological relevance (Caizzo and Baldwin, 1997; James et al., 1996). However, the recorded times to peak twitch force and times to half peak tetanus force (Fig. 3) were significantly correlated with the cycle frequencies for optimal power output in our data (N=40, r^2=0.41 and 0.35, respectively, P<0.0001). As the same differences between the three muscles (Fig. 1) were observed in each of these three variables, our data suggest that ontogenetic changes in relatively simple measurements such as twitch or tetanus rise times can already be indicative of size-related changes during work-loop experiments, which more closely reflect the *in vivo* dynamic conditions of the muscles.

It should be noted that certain morphological modifications may help reduce the extent to which the contractile properties need to be adjusted during ontogeny in order to keep muscles working at the plateau of the power–speed curve during feeding. The latter can only be accomplished if the muscle shortening rate $\Delta L/(L_0\Delta t)$ remains constant for animals of different sizes, with time increment Δt inevitably increasing with body size due to the biomechanical consequences of scaling (Hill, 1950; Van Wassenbergh et al., 2005a). This can either be done by (1) negative allometric growth of muscle length L_0 or by (2) positive allometry in the total length change of the muscle ΔL for a given movement. The first solution

seems to occur in the catfish *Clarias gariepinus*, where fibre lengths of some cranial muscles show a slight negative allometry (Herrel et al., 2005) while the length of the moment arms of the jaw system and the magnitude of excursion of the cranial elements during feeding scale approximately isometrically (Van Wassenbergh et al., 2005a). Note that this means the slope of the scaling model prediction line may actually be less steep than shown in Fig. 5, which would result in the model predictions corresponding even better to the frequencies for optimal power output measured *in vitro*.

The second option seems to occur in the sunfishes *Lepomis punctatus* and *Lepomis macrochirus*, for which both the in-levers and out-levers of the lower jaw scale with positive allometry (Wainwright and Shaw, 1999). This means that if the rest of the feeding apparatus grows isometrically, a given rotation of the lower jaw will cause a relatively larger length change in the muscles that cause mouth opening and mouth closing. Therefore, similar to the catfish, a small increase in the strain of the muscle fibres $\Delta L/L_0$ during ontogeny may occur in these sunfishes, which potentially helps the fish to produce maximal power during feeding over a wider range of body sizes. Consequently, the speed of contraction of the muscle fibres will decrease less rapidly with size. Obviously, only limited changes in muscle strain during ontogeny are possible due to the force–length relationship of muscle. Therefore, we hypothesise that the physiological changes manifested in the negative scaling of the cycle frequency for optimum power output (Fig. 5) are more important to maintain optimal power output compared with morphological modifications increasing ΔL or decreasing L_0 in the course of ontogeny.

Irrespective of scaling relationships, the three muscles analyzed in the present study differ in several contractile properties. An example of these is the significantly lower cycle frequency for maximal power output for the m-a-m compared to the m-pr-h (Fig. 6B,C). Interestingly, this is in accordance with the natural behaviour of these muscles: the m-pr-h, used for fast mouth opening, generally shows higher contraction velocities compared with the jaw adductor muscle (m-a-m) during feeding, and this is reflected in the force–speed relationship of the muscle. In addition, the latter muscle is also used for exerting static bite force onto prey (Herrel et al., 2002). Our study therefore showed that fast-fibred muscle of the feeding system cannot be regarded as ‘similar’ with reference to their contractile physiology. Because the observed differences in *in vitro* contractile properties between different muscles matched our expectations based on *in vivo* measurements of feeding kinematics (Van Wassenbergh et al., 2005b), these results suggest that, within a single species, muscle physiology can be fine-tuned to relatively small differences in the contractile regime of a muscle. However, as considerably larger differences between contractile properties of a specific muscle from small and large catfish were observed, our study particularly emphasises the importance of the effects of scaling for the mechanics of musculo-skeletal systems at the level of muscle physiology during ontogeny.

Thanks to F. Ollevier, F. Volckaert and E. Holsters for providing us with the largest individuals used in this study. W. Fleuren is acknowledged for supplying all other *C. gariepinus* specimens. Thanks to Mark Bodycote for technical assistance, and the two anonymous reviewers for their helpful comments. The authors gratefully acknowledge support of the Special Research Fund of the University of Antwerp. S.V.W. and A.H. are postdoctoral fellows of the fund for scientific research – Flanders (FWO-Vl).

References

Adriaens, D., Aerts, P. and Verraes, W. (2001). Ontogenetic shift in mouth opening mechanisms in a catfish (Clariidae, Siluriformes): a response to increasing functional demands. *J. Morphol.* **247**, 197-216.

Aerts, P., Osse, J. W. M. and Verraes, W. (1987). Model of jaw depression during feeding in *Astatotilapia elegans* (Teleostei: Cichlidae). Mechanisms for energy storage and triggering. *J. Morphol.* **194**, 85-109.

Altringham, J. D. and Ellerby, D. J. (1999). Fish swimming: patterns in muscle function. *J. Exp. Biol.* **202**, 3397-3403.

Altringham, J. D. and Johnston, I. A. (1990). Scaling effects on muscle function: power output of isolated fish muscle fibres performing oscillatory work. *J. Exp. Biol.* **151**, 453-467.

Altringham, J. D., Morris, T., James, R. S. and Smith, C. I. (1996). Scaling effects on muscle function in fast and slow muscles of *Xenopus laevis*. *Exp. Biol. Online* **1**, 6.

Anderson, M. E. and Johnston, I. A. (1992). Scaling of power output in fast muscle fibres of the Atlantic cod during cyclical contraction. *J. Exp. Biol.* **170**, 143-154.

Biewener, A. A. (2005). Biomechanical consequences of scaling. *J. Exp. Biol.* **208**, 1665-1676.

Caizzo, V. J. and Baldwin, K. M. (1997). Determinants of work produced by skeletal muscle: potential limitations of activation and relaxation. *Am. J. Physiol. Cell Physiol.* **273**, C1049-C1056.

Carroll, A. M. and Wainwright, P. C. (2006). Muscle function and power output during suction feeding in largemouth bass, *Micropterus salmoides*. *Comp. Biochem. Physiol.* **143A**, 389-399.

Carroll, A. M., Wainwright, P. C., Huskey, S. H., Collar, D. C. and Turingan, R. G. (2004). Morphology predicts suction feeding performance in centrarchid fishes. *J. Exp. Biol.* **207**, 3873-3881.

Cook, A. (1996). Ontogeny of feeding morphology and kinematics in juvenile fishes: a case study of the cottid fish *Clinocottus analis*. *J. Exp. Biol.* **199**, 1961-1971.

Coughlin, D. J. and Carroll, A. M. (2006). *In vitro* estimates of power output by epaxial muscle during feeding in largemouth bass. *Comp. Biochem. Physiol.* **145A**, 533-539.

Curtin, N. A. and Woledge, R. C. (1988). Power output and force-velocity relationship of live fibres from white myotomal muscle of the dogfish *Scyliorhinus canicula*. *J. Exp. Biol.* **140**, 187-197.

Deban, S. M. and O’Reilly, J. C. (2005). The ontogeny of feeding kinematics in a giant salamander *Cryptobranchus alleganiensis*: does current function or phylogenetic relatedness predict the scaling patterns of movement? *Zoology* **108**, 155-167.

Diogo, R., Oliveira, C. and Chardon, M. (2001). On the osteology and mycology of catfish pectoral girdle, with a reflection on catfish (Teleostei: Siluriformes) plesiomorphies. *J. Morphol.* **249**, 100-125.

Hernandez, L. P. (2000). Intraspecific scaling of feeding mechanics in an ontogenetic series of zebrafish, *Danio rerio*. *J. Exp. Biol.* **203**, 3033-3043.

Hernandez, L. P. and Motta, P. J. (1997). Trophic consequences of differential performance in the sheepshead, *Archosargus probatocephalus* (Teleostei, Sparidae). *J. Zool. Lond.* **243**, 737-756.

Herrel, A. and Gibb, A. (2006). Ontogeny of performance. *Physiol. Biochem. Zool.* **79**, 1-6.

Herrel, A., Adriaens, D., Verraes, W. and Aerts, P. (2002). Bite performance in clariid fishes with hypertrophied jaw adductors as deduced by bite modelling. *J. Morphol.* **253**, 196-205.

Herrel, A., Van Wassenbergh, S., Wouters, S., Adriaens, D. and Aerts, P. (2005). A functional morphological approach to the scaling of the feeding system in the African catfish, *Clarias gariepinus*. *J. Exp. Biol.* **208**, 2091-2102.

Hill, A. V. (1950). The dimensions of animals and their muscular dynamics. *Sci. Prog. Lond.* **38**, 209-230.

Hossain, M. A. R., Batty, R. S., Haylor, G. S. and Beveridge, M. C. M. (1999). Diel rhythms of feeding activity in African catfish, *Clarias gariepinus* (Burchell 1822). *Aquac. Res.* **30**, 901-905.

James, R. S. and Johnston, I. A. (1998). Scaling of muscle performance during escape responses in the fish *Myoxocephalus scorpius* L. *J. Exp. Biol.* **201**, 913-923.

James, R. S., Young, I. S., Cox, V. M., Goldspink, D. F. and Altringham, J. D. (1996). Isometric and isotonic muscle properties as determinants of work loop muscle power output. *Pflügers Arch.* **432**, 767-774.

James, R. S., Cole, N. J., Davies, M. L. F. and Johnston, I. A. (1998). Scaling of intrinsic contractile properties and myofibrillar protein composition of fast muscle in the fish *Myoxocephalus scorpius* L. *J. Exp. Biol.* **201**, 901-912.

Josephson, R. K. (1985). Mechanical power output from striated muscle during cyclic contraction. *J. Exp. Biol.* **114**, 493-512.

Lauder, G. V. (1985). Aquatic feeding in lower vertebrates. In *Functional Vertebrate Morphology* (ed. M. Hildebrand, D. M. Bramble, K. F. Liem and D. B. Wake), pp. 210-229. Cambridge, MA: The Belknap Press, Harvard University Press.

Medler, S. (2002). Comparative trends in shortening velocity and force production in skeletal muscles. *Am. J. Physiol.* **283**, R368-R378.

Mendez, J. and Keys, A. (1960). Density and composition of mammalian muscle. *Metabolism* **9**, 184-188.

Meyers, J. J., Herrel, A. and Birch, J. (2002). Scaling of morphology, bite force and feeding kinematics in an Iguanian and a Scleroglossan lizard. In *Topics in Functional and Ecological Vertebrate Morphology* (ed. P. Aerts, K. D'Août, A. Herrel and R. Van Damme), pp. 47-62. Maastricht: Shaker Publishing.

Reilly, S. M. (1995). The ontogeny of aquatic feeding behavior in *Salamandra salamandra*: stereotypy and isometry in feeding kinematics. *J. Exp. Biol.* **198**, 701-708.

Richard, B. A. and Wainwright, P. C. (1995). Scaling the feeding mechanism of largemouth bass (*Micropterus salmoides*): kinematics of prey capture. *J. Exp. Biol.* **198**, 419-433.

Robinson, M. P. and Motta, P. J. (2002). Patterns of growth and the effects of scale on the feeding kinematics of the nurse shark (*Gynglymostoma cirratum*). *J. Zool. Lond.* **256**, 449-462.

Rome, L. C. and Sosnicki, A. A. (1991). Myofilament overlap in swimming carp. II. Sarcomere length changes during swimming. *Am. J. Physiol.* **260**, C289-C296.

Schmidt-Nielson, K. (1984). *Scaling: Why is Animal Size so Important?* Cambridge: Cambridge University Press.

Sokal, R. F. and Rohlf, F. J. (1995). *Biometry*. New York: W. H. Freeman.

Thys, T. (1997). Spatial variation in epaxial muscle activity during prey strike in largemouth bass (*Micropterus salmoides*). *J. Exp. Biol.* **200**, 3021-3031.

Van Wassenbergh, S., Aerts, P. and Herrel, A. (2005a). Scaling of suction-feeding kinematics and dynamics in the African catfish, *Clarias gariepinus*. *J. Exp. Biol.* **208**, 2103-2114.

Van Wassenbergh, S., Herrel, A., Adriaens, D. and Aerts, P. (2005b). A test of mouth-opening and hyoid-depression mechanisms during prey capture in a catfish. *J. Exp. Biol.* **208**, 4627-4639.

Van Wassenbergh, S., Aerts, P., Adriaens, D. and Herrel, A. (2005c). A dynamical model of mouth closing movements in clariid catfishes: the role of enlarged jaw adductors. *J. Theor. Biol.* **234**, 49-65.

Van Wassenbergh, S., Aerts, P. and Herrel, A. (2006). Scaling of suction feeding performance in the catfish *Clarias gariepinus*. *Physiol. Biochem. Zool.* **79**, 43-56.

Wainwright, P. C. and Shaw, S. S. (1999). Morphological basis of kinematic diversity in feeding sunfishes. *J. Exp. Biol.* **202**, 3101-3110.

Wainwright, P. C., Huskey, S. H., Turingan, R. G. and Carroll, A. M. (2006). Ontogeny of suction feeding capacity in snook, *Centropomus undecimalis*. *J. Exp. Zoolog. Part A Comp. Exp. Biol.* **205**, 246-252.

Wakeling, J. M. and Johnston, I. A. (1998). Muscle power output limits fast-start performance in fish. *J. Exp. Biol.* **201**, 1505-1526.

Wakeling, J. M. and Johnston, I. A. (1999). Predicting muscle force generation during fast-starts for the common carp *Cyprinus carpio*. *J. Comp. Physiol. B* **169**, 391-401.